TÜBİTAK

Turkish Journal of Biology

http://journals.tubitak.gov.tr/biology/

Research Article

Turk J Biol
(2017) 41: 796-807

doi:10.3906/biy-1704-31

N-Acetylglucoseamine modified alginate sponges as scaffolds for skin tissue engineering

Murat DEMİRBİLEK[1,*], Nelisa TÜRKOĞLU LAÇİN[2], Selçuk AKTÜRK[3]

[1]Advanced Technologies Research and Application Center, Hacettepe University, Ankara, Turkey
[2]Science and Technology Application and Research Center, Yıldız Technical University, İstanbul, Turkey
[3]Department of Physics, Faculty of Science, Muğla Sıtkı Koçman University, Muğla, Turkey

Received: 14.04.2017 • **Accepted/Published Online:** 04.07.2017 • **Final Version:** 10.11.2017

Abstract: In the treatment of dermal wounds, wound-dressing materials prepared from natural mucopolysaccharides are widely used because of their advantages such as nonirritation, nontoxicity, and ease in topical application. In the present study, alginate hydrogels modified with N-acetyl glucose amine (NAG) were prepared as wound-dressing material. Physical, chemical, thermal, and mechanical properties of the hydrogels were studied. Cytotoxicity of the hydrogels on endothelial (HUVEC) and keratinocyte (HaCaT) cells were examined. Anti- and proinflammatory cytokine levels of human monocyte-macrophage cells (THP-1) stimulated with hydrogels were determined. According to the results, increasing the NAG concentration led to an increase in the swelling and nitrogen ratios in the hydrogels. Additionally, increasing the NAG concentration decreased elastic modulus and degradation time. Hydrogels were not cytotoxic on HaCaT and HUVEC cells. It stimulated IL-10 and TNF-alpha levels at a small rate.

Key words: Biomaterials, alginate hydrogels, hyaluronic acid monomers, cytokines

1. Introduction

After trauma or surgery, the disruption of the normal anatomical and functional integrity of the skin is called a wound. Some postinjury events are intended to restore tissue integrity regarding functional and anatomical features. All of these events are called wound healing. Wound healing includes hemostasis, inflammation, proliferation, and remodeling phases (Demidova-Rice et al., 2012).

Hyaluronic acid (HA) is a mucopolysaccharide. The monomers are N-acetyl glucosamine (NAG) and D-glucuronic acid (D-GA) (Jahn et al., 1999). It is mainly involved in the proteoglycan structure in the amorphous extracellular matrix. It is also found in the vitreous fluid of the eyes and synovial fluid of the joints in free form. HA is particularly important during the inflammation and epithelialization phases of the wound-healing process (Ates et al., 2004). HA stimulates the phagocytic activity of neutrophils and macrophages and increases the release of chemotactic factors from fibroblasts. In fetal wounds, the addition of HA degradation products was shown to increase fibrosis (Olutoye and Cohen, 1996). In addition to being an extracellular matrix element, HA is present in cell cytoplasm because of its role in the regulation of nucleus function (Croce et al., 2003). Some studies showed that exogenous high molecular weight HA addition inhibits cell proliferation and functions. Croce et al. reported that exogenous high molecular weight HA did not induce HA synthesis. At the same time, they found that exogenous high molecular weight HA reduces total protein and collagen synthesis (2001). Sheehan et al. demonstrated that high concentration of high molecular weight HA induces apoptosis in U937 cells (2004). It is thought that with an alginate–NAG graft this disadvantage of high molecular weight HA can be avoided.

Commercially, there are alginate wound dressings containing silver, growth factors, or HA. Alginate is a mucopolysaccharide and consists of β-D-mannuronic acid and α-L-guluronic acid (Draget et al., 1997). Alginate wound dressings have ion-exchange properties. In contact with the wound, the calcium ions in the chains are replaced by sodium ions in the body fluid. As a result, part of the chain becomes sodium alginate. This ion exchange allows the sheath to swell and cause gel formation on the wound surface. Because of this feature, alginate is an ideal material for the production of moisturizing wound dressings (Soares et al., 2004). The swelling ability of the alginate wound dressing allows for excess fluid trapping at the wound surface and prevents the wound from dehydrating (Wiegand et al., 2009). In an in vivo transdermal wound-

* Correspondence: muratscaffold@gmail.com

healing model, Kataria et al. found that ciprofloxacin-loaded PVA-alginate nanofibers increased the amount of hydroxyproline (2014).

High level of proinflammatory cytokines, especially IL-1 and IL-6 and TNF-alpha, exacerbate inflammation in wound healing. IL-1 is produced by neutrophils, monocytes, macrophages, and keratinocytes. In addition to having a paracrine effect, autocrine activity enhances keratinocyte migration and proliferation. IL-1 activates fibroblasts and increases FGF-7 release (Komine et al., 2000). IL-6 is produced by neutrophils and monocytes and has been shown to be important in initiating the healing process (Grellner et al., 2000). It has also been demonstrated that the synthesis continues in old wounds. IL-6 has a proliferative effect on keratinocytes and is a chemoattractant to neutrophils (Werner et al., 1992). TNF-alpha stimulates epithelialization in wound healing on FGF-7. At low levels, TNF-alpha indirectly stimulates inflammation and may promote wound healing by increasing growth factors produced by macrophages. However, at higher levels, TNF-alpha delays healing because of induced inflammation (Wallace and Stacey, 1998). In one study, TNF-alpha and IL-1b stimulated the synthesis of metalloproteinase, such as collagenase, and hyaluronidase in chronic wounds, and the extent of inflammation in chronic wounds was linked to this synthesis (Unemori et al., 1991).

The purpose of the present study was to prepare alginate wound-dressing materials modified with NAG and to perform biocompatibility tests.

2. Materials and methods

2.1. Preparation and characterization of hydrogels

In the present study, NAG-modified alginate hydrogels were prepared and characterized. For this purpose, 2% alginate solution was prepared, and the pH values of the solutions were adjusted to 10 with 1 M NaOH. NAG was added to the solutions at ratios of 0%, 2%, 5%, and 10% (w/w alginate), designated as Alg, Alg-2, Alg- 5, and Alg-10, respectively, according to the percent NAG concentrations added to the formulations. Once homogenization of the solution was achieved, it was poured into petri dishes. It was stored at –80 °C overnight and then lyophilized for 2 days at –80 °C. The hydrogel was exposed to epichlorohydrin vapor at 15 mmHg pressure at 50 °C for cross-linking of NAG and alginate (Fundueanu et al., 1999; Chang et al., 2009). pH values of the crosslinked hydrogels were neutralized by washing with deionized water. After washing, the hydrogels were re-freeze–dried and stored at 4 °C (Sinha et al., 2013).

2.2. Chemical characterization of hydrogels

Infrared spectra of the Alg, Alg-2, Alg-5, and Alg-10 hydrogels, both crosslinked with epichlorohydrin and not, were obtained, with a resolution of 4 cm^{-1} over the 400–4000 cm^{-1} spectral range. For this purpose, an attenuated total reflection (ATR) attached Fourier transform infrared (FTIR) spectrophotometer (Thermo Scientific, Nicolet iS50) was used.

2.3. Morphological characterization of hydrogels

The surface porosity and texture of hydrogels were determined by scanning electron microscopy (SEM; JSM–7600 F, Jeol, Tokyo, Japan) analyses. For this purpose, the scaffolds were covered with gold and SEM photographs were taken under low voltage. The nitrogen content of samples was determined using the energy dispersive X-ray spectroscopy (EDS; Oxford Instruments, Abingdon, UK) attachment. Total pore ratios of the hydrogels were determined by microcomputed tomography (micro-CT). For this purpose, hydrogels were scanned using Bruker, Sky Scan 1272 X-ray micro-CT at Hacettepe University, HUNITEK (Advanced Technologies Research and Application Center), Ankara, Turkey. Optimal scanning parameters for all tiny samples (approximately 3 mm width, 2 mm height) were set up to obtain an appropriate contrast between air and matrix material without beam-hardening artifacts on pore boundaries. Each hydrogel was scanned under the following conditions: no filter, 3 frame averaging, 0.3 rotational step options, 1 h exposure, 200 μA, 50 kV X-ray emission. During the scan, radiographic projections were captured using 3 K binning (1632 × 1092 pixels) on the CCD camera, applying a 665 ms exposure time for each rotational step. After the scan, a total of 876 16-bit 1632 × 1092 pixel raw radiographic projection images were reconstructed to 8-bit 1412 × 1412 pixel bitmap images using NRecon software. The reconstructed 2-D image slices were processed using the CT analyzer (CTAn) software package to segment and construct a complete 3-D reconstruction (volume rendering) for each scaffold. Pores in 2-D images were segmented from a solid matrix based upon simple grayscale thresholding via contrast difference having different density materials. Segmented parts of the scaffolds were monitored as 3-D volume using CTVox software. Volume rendering displays provided visualization of the internal structure of each sample and were used for qualitative inspection of the 3-D geometry of pore shape characteristics and also for investigation of the heterogeneity in the solid matrix.

2.4. Swelling analysis of hydrogels

Swelling tests were carried out to determine the water-holding capacities of the hydrogels. The dry weights (W_0) of the hydrogels were measured. Then the hydrogels were inserted into 10 mL of PBS (pH 7.4) at 37 °C. Samples were removed from the buffer after 15, 30, 60, and 90 min, and their weights were determined (Ws). The water retention rate of the samples was calculated using the following equation. The studies were carried out with three parallel samples.

$$\text{Swelling ratio} = (Ws - W_0)/W_0$$

2.5. Degradation analysis of hydrogels

The in vitro degradation profile of hydrogels was determined by the gravimetric method. Three parallel samples were used in the study. The dry weights (W_0) of the hydrogels were determined. They were incubated in PBS buffer at 37 °C for 15 days. At the end of 15 days, the samples were washed with distilled water, then dried in a lyophilizer (Alpha 2-4 LD; Martin Christ Gefriertrocknungsanlagen, Osterode am Harz, Germany) and then weighed (W). The deformation values of the scaffolds were calculated by the following formula. The results are given as percent weight loss.

$$\text{Weight loss (\%)} = [(W_0 - W)/W_0] \times 100$$

2.6. Thermal analysis of hydrogels

Thermograms of hydrogels were analyzed by differential scanning colorimetry (DSC). For this purpose, 10-µg samples were placed in a pan and heated from 25 °C to 400 °C at a rate of 10 °C per min under nitrogen gas. Melting temperatures and enthalpies of the samples were calculated.

2.7. Mechanical analysis of hydrogels

The mechanical properties of the hydrogels were determined using an AG-IS (Z250 universal testing machine; Zwick Roell, Ulm, Germany). The study was performed in room conditions. Specimens measuring 0.2 × 2 × 5 cm (thickness × width × length) were clamped to the device clamps, and the device was set to a pull speed of 5 mm/min.

2.8. In vitro studies

The cytotoxicity of the hydrogels was examined with human endothelial (HUVEC) and keratinocyte (HaCaT) cells. For this purpose, HUVEC and HaCaT cells were cultured at 37 °C in DMEM-F12 medium containing 10% FCS and 1% L-glutamine in a 5% carbon dioxide atmosphere. Hydrogels were cut into discs and placed in 48-well plates. A 70% ethanol–water solution sterilized by injector filtration was added onto the hydrogels. They were sterilized under UV light for 2 h. After sterilization, the hydrogel was washed several times with pH 7.4, 0.1 M PBS.

Cytotoxicity of hydrogels was determined via indirect cytotoxicity. For this purpose, 0.2 g/mL hydrogels were incubated for 72 h in a 5% carbon dioxide incubator at 37 °C in a cell culture medium. Endothelial and keratinocyte cells were seeded individually in 96-well plates at a concentration of 3000 cell/mL and left for incubation at 37 °C with 5% carbon dioxide. After overnight incubation, the media were discarded and 100 µL of media containing 10 µL MTT solution (25 mg/mL, dissolved in pH 7.4, 0.1 M PBS) was pipetted onto the cells. The plates were incubated for 4 h. The media were discarded, and 100 µL of HCl-isopropanol solution was pipetted onto the hydrogels to dissolve the resulting formazan crystals and then their absorbance was read at 570 nm.

THP-1 cells were plated into 24-well plates at a concentration of 3000 cells/mL and 20 ng/mL of a phorbol 12-myristate 13-acetate (PMA) was pipetted onto the cells for 3 days. The transformation of cells into macrophages was examined by light microscopy (Figure 1). Hydrogels were cut into disks of 0.5 cm in diameter and then placed in the wells, and the plate was incubated at 37 °C with 5% carbon dioxide for 2 days. After the end of incubation, the cell culture medium was removed and centrifuged at 5000 rpm. IL-10 and TNF-alpha levels were determined using commercial kits.

2.9. Statistical analysis

Six samples for each cell culture experimental group were used. Each analysis was triplicated. Numerical data were analyzed using column analysis and nonparametric t-test in GraphPad 6. $P < 0.005$ was considered statistically significant.

3. Results and discussion

Many commercial forms of alginate wound-dressing materials are available on the market. This study, contrary to commercial forms, aimed to prepare a wound dressing similar to HA, which is an extracellular matrix amorphous ground material. For this purpose, alginate hydrogels with and without NAG (Alg, Alg-2, Alg-5, and Alg-10) were prepared for use as a wound dressing. Physical characterization of hydrogels was performed via SEM and micro-CT studies, chemical characterization was

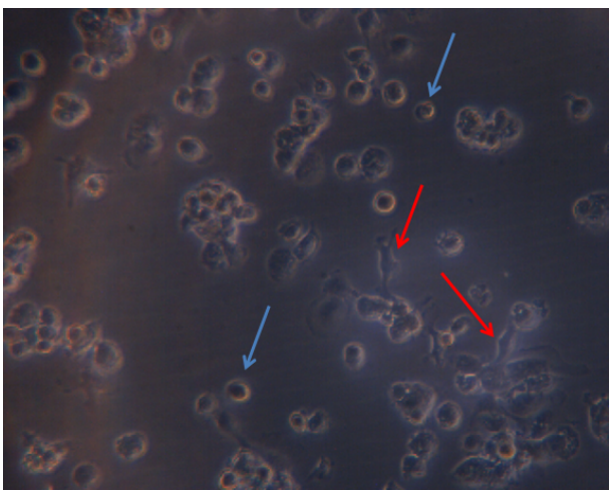

Figure 1. Monocyte (spherical) cells were converted to macrophages (hold the plate with pseudopod and flat shape) using PMA. The photograph was taken at hour 24 of the PMA application.

performed via ATR-FTIR studies, thermal properties were determined via DSC analysis, and mechanical properties were determined via a universal test machine. Cytotoxicity of human skin cells on keratinocyte and endothelial cells was investigated. The effect of hydrogels on anti- and proinflammatory cytokine levels was measured using THP-1 cells.

Alginate hydrogels including different active substances, such as polypeptides (Hashimoto et al., 2004) and antibacterial drugs (Kim et al., 2008), have been prepared for use in wound healing and tested under in vitro and in vivo conditions. Alginate blend hydrogels, such as gelatin (Balakrishnan et al., 2005) and carboxymethyl cellulose (Walker et al., 2003), were also prepared and tested. Alginate has advantages as a wound-dressing material. As a result of histamine activity of the mast cells in the wound area, severe edema occurs. Alginate hydrogels, due to their high water retention capacities, reduce edema and also pain (Asada et al., 1997). Ionic cross-linked alginate hydrogels have a high rate of degradation in the wound area (Das and Pal, 2015). The scar tissue receives calcium ions and weakens the cross-linking ratio of the hydrogel. This property gives the alginate matrix an advantage when it comes to amorphous wounds. In the study, the alginate hydrogel was cross-linked with epichlorohydrin. Compared to ionic cross-linking, the structure imparts more flexibility and longer degradation properties (Lee and Mooney, 2012). Chang et al. (2009) schematized cross-linking mechanism of alginate and cellulose. Moreover, Laus et al. (2010) schematized cross-linking mechanism of chitosan. They both demonstrated that polysaccharides were cross-linking via carboxylic acid groups with epichlorohydrin.

3.1. Morphological analysis of hydrogels

SEM studies have shown that hydrogels have a complex structural porosity. The pore sizes of the Alg, Alg-2, Alg-5, and Alg-10 hydrogels were 97.54 ± 8.31, 95.38 ± 14.0, 92.34 ± 11.9, and 100.74 ± 13.65 μm, respectively, according to SEM. Li et al. (2005) formed alginate–chitosan blend hydrogels with a pore size of 100–300 μm, while Mohan and Nair (2005) recorded an alginate sponge pore size of 25–350 μm; both studies ionically cross-linked their sponges, resulting in a range of pore sizes. In this study, the hydrogels are covalently bonded and the pore size changes in a narrow range.

Total porosity and open and closed porosity of hydrogels were determined by micro-CT. When the results were examined, increased NAG concentrations decreased the cross-linking rate of alginate chains. Therefore, increased NAG concentrations increased total and open porosity and reduced closed porosity. The total porosity values for Alg, Alg-2, Alg-5, and Alg-10 hydrogels were 57.05%, 59.9%, 68.2% and 72.3%, respectively, according to micro-CT. SEM, micro-CT, and macroscopic photographs of the hydrogels are presented in Figure 2. Micro-CT results are presented in Table 1.

The nitrogen content of hydrogels was determined by EDS. According to the results (Figure 3), the highest amount of nitrogen was seen in Alg-10. The ratio of nitrogen in hydrogels increased with the increasing NAG ratio (Maia et al., 2013).

3.2. Chemical characterization of hydrogels

IR spectra of the Alg, Alg-2, Alg-5, and Alg-10 hydrogels with and without cross-linking (Figure 4) were obtained. At all hydrogel spectra, O–H stretches were seen at 3000–3400 cm^{-1}. Aliphatic C–H stretches were seen at 2926 cm^{-1}. C=O stretches were seen at 1594–1613 cm^{-1}. C–H blends were seen at 1450 cm^{-1}. C–O bonds for acid groups were seen at 1230 cm^{-1}. At 1080 cm^{-1}, secondary and tertiary alcohol blends were seen (Trif et al., 2007; Harper, 2013). In cross-linked hydrogel spectra, cyclic epoxy bonds belonging to free epichlorohydrin at 1250 cm^{-1}, with moderate intensity, were not observed (Zhang and Jia, 2010). C–O–C bonds at 810–950 cm^{-1} and at 750–840 cm^{-1} overlapped with C–O–C bonds in alginate hydrogels.

3.3. Swelling analysis of hydrogels

Ionic or covalent cross-linking alters the swelling capacity of alginate hydrogels. Straccia et al. (2015) found that hydrogels crosslinked with 1% calcium ions swelled 400% and when the calcium concentration was lowered to 2%, the hydrogels showed 200% swelling. In the present study, hydrogels were chemically cross-linked by epichlorohydrin and the swelling results (n = 3) are given in Figure 5A. The swelling rates of the Alg, Alg-2, Alg-5, and Alg-10 hydrogels were 468.5 ± 26.8%, 484.37 ± 24.0%, 512.98 ± 22.7%, and 647.82 ± 31.7%, respectively, after 30 min. After 90 min, those values were 494.5 ± 39.4%, 525 ± 37.7%, 551.98 ± 35.9%, and 717.39 ± 39.7%, respectively. The swelling ratio of the tissue scaffolds reached a plateau after about 30 min and the swelling ratio of Alg-10 was the highest. This shows that NAG enters between the polymer chains and that the chain structure is looser than Alg. However, according to results obtained by Catanzano et al. (2015), the amount of hyaluronic acid has a minimum effect on hydrogel swelling capacity.

3.4. Degradation analysis of hydrogels

Control of the degradation properties of a scaffold is a matter that affects the regeneration processes of different tissues due to tissue-specific cellular activities. In this respect, the degradation properties of scaffolds prepared for various tissues and different purposes are of great importance. Simmons et al. (2004) noted that growth factors, scaffold properties, and their appropriate combinations play a critical role in bone tissue regeneration. In another study, hydrogels prepared at a ratio of 1:1 took longer to degrade than those prepared at a ratio of 1:2 (Hsu et al., 2004). In the present study, degradation profiles of hydrogels were

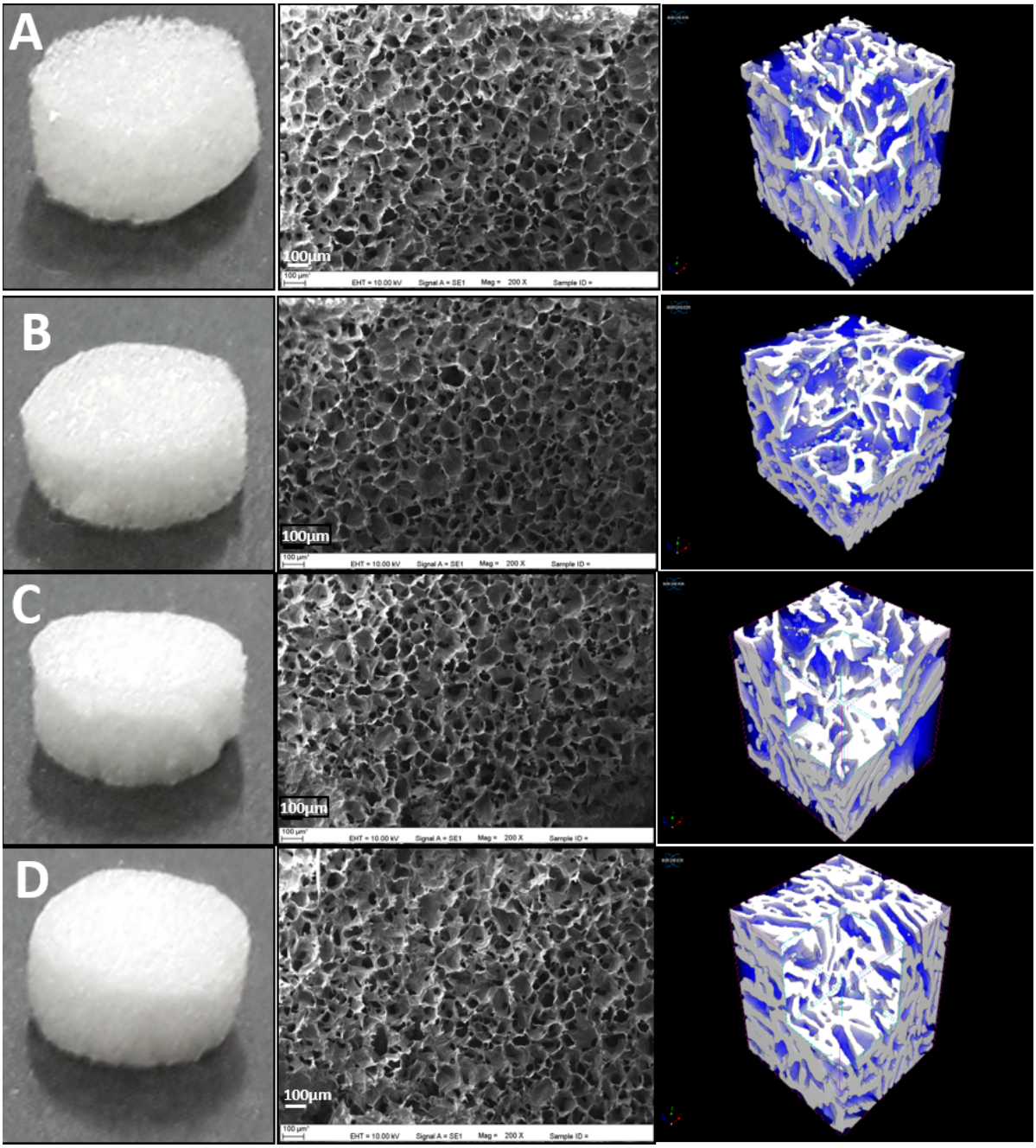

Figure 2. Macroscopic, SEM, and micro-CT photographs of Alg (A), Alg-2 (B), Alg-5 (C), and Alg-10 (D) hydrogels.

determined by gravimetric method (n = 3). The results are presented in Figure 5B. Alginate hydrogel degradation was slower than hydrogels containing NAG. NAG cross-linked to alginate chains has been shown to reduce the cross-linking rate.

3.5. Thermal analysis of hydrogels

The thermal properties of the hydrogels were determined by DSC. The DSC curves and temperature values of the peaks are given in Figure 6. Endothermic dehydration peaks were observed between 71.72 and 104.46 °C. It was determined that the highest dehydration value was in the Alg-10 hydrogel and the dehydration temperature increased with increasing NAG concentration. An endothermic peak at 209.0–229.8 °C and narrower exothermic depolymerization peaks at 258.5–280.0 °C were observed in the thermogram. Soares et al. (2004)

Table 1. Total, open, and closed porosity of Alg, Alg-2, Alg-5, and Alg-10 hydrogels were determined by micro-CT.

	Closed porosity (%)	Open porosity (%)	Total porosity (%)
Alg	0.026	57.042	57.053
Alg-2	0.024	63.887	59.906
Alg-5	0.020	68.278	68.284
Alg-10	0.011	72.327	72.330

found that the dehydration temperature of alginate varied between 75 and 96 °C. Draget et al. (1997) observed a small endothermic peak at 190 °C and a sharp exothermic peak at 300 °C of depolymerization. Sarmento et al. (2006) also detected peaks of dehydration between 62 and 86.6 °C of alginate. Simmons et al. (2004) detected two exothermic peaks of depolymerization at 247.8 and 311.0 °C.

3.6. Mechanical analysis of hydrogels

Since the mechanical properties of hydrogels directly affect cellular activities, mechanical properties influence cell proliferation, spreading, and functions (Chaudhuri et al., 2015). Mechanical analysis results of the hydrogels are given in Table 2. According to the results, elongation at break (%) increased with increasing NAG concentration. Alg-10 had the highest elastic modulus. Kaklamani et al. (2014) determined that increasing polymer concentration on hydrogels increases elastic modulus.

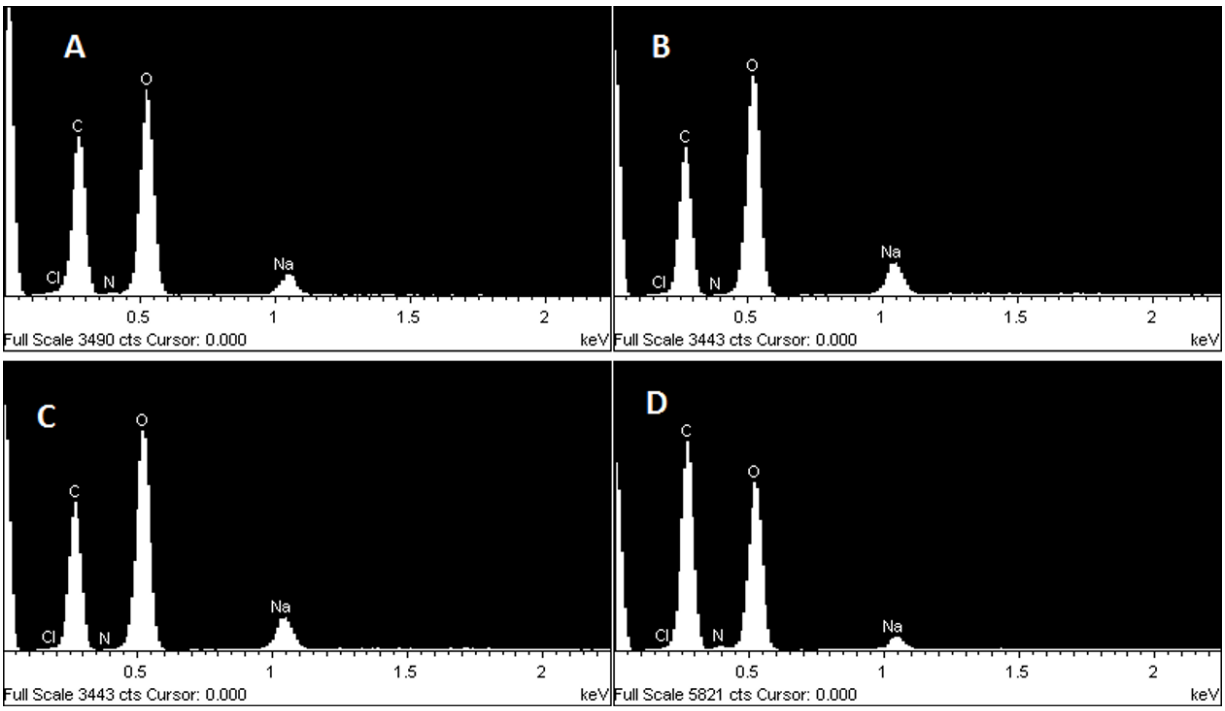

	Alg		Alg-2		Alg-5		Alg-10	
Elements	Weight (%)	Atomic (%)	Weight (%)	Atomic (%)	Weight (%)	Atomic (%)	Weight (%)	Atomic (%)
C	37,24	45,25	38,08	45,77	39,77	47,65	43,81	51,10
N	0,32	0,33	0,67	0,70	1,28	1,31	3,86	3,85
O	55,07	50,29	56,2	50,63	53,07	47,74	50,12	43,89
Na	4,89	3,11	3,78	2,38	4,15	2,60	1,37	0,83
Cl	2,48	1,02	1,27	0,52	1,73	0,70	0,84	0,33

Figure 3. Distributions of C, N, O, Na, and Cl atoms in Alg (A), Alg-2 (B), Alg-5 (C), and Alg-10 (D) hydrogels were determined by EDS analysis.

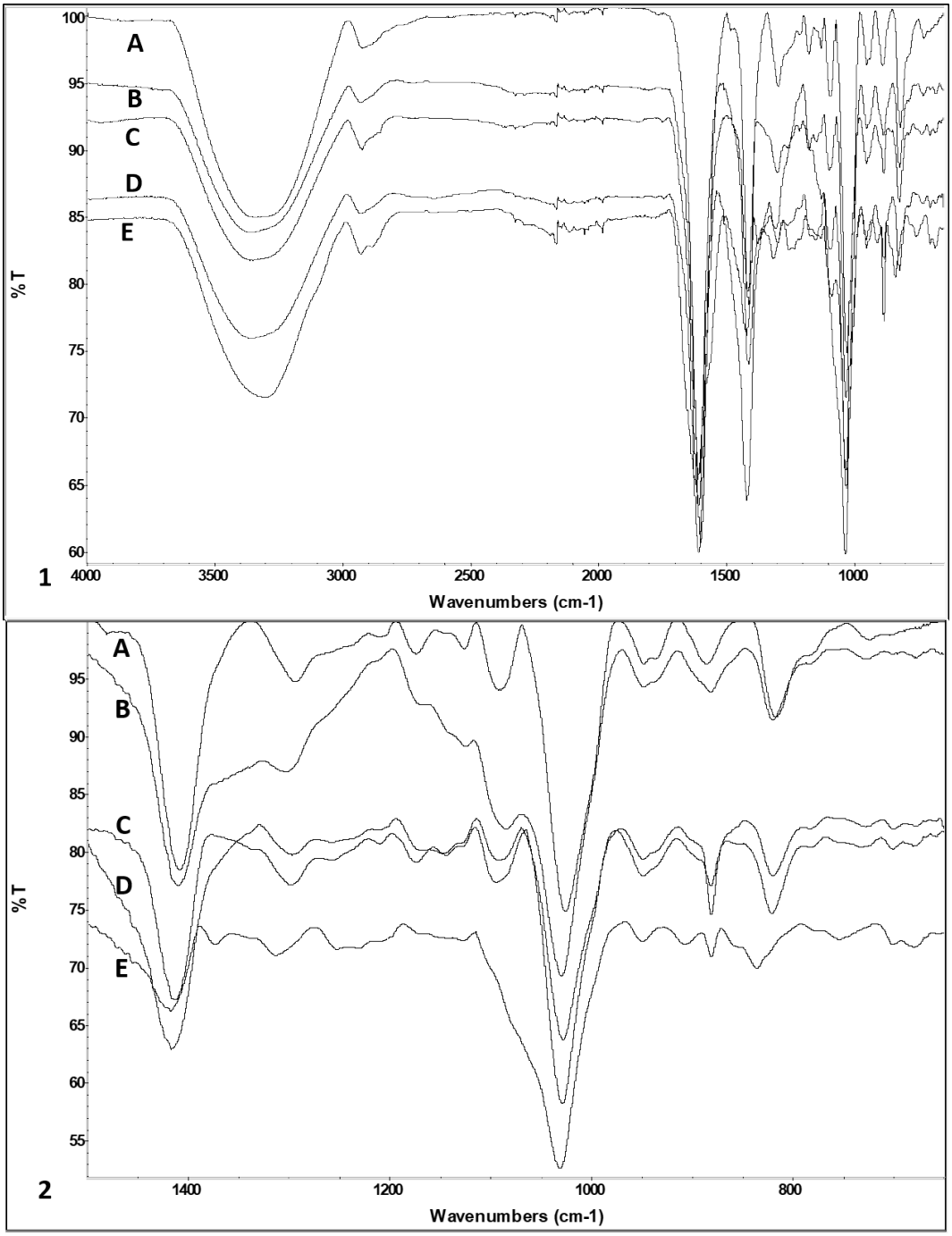

Figure 4. ATR-FTIR spectra of Alg (A), Alg-2 (B), Alg-5 (C), and Alg-10 (D) hydrogels; spectral range between 400 and 4000 cm^{-1} (1) and 650 and 1500 cm^{-1} (2).

Harper et al. (2013) prepared alginate blend films with different polysaccharides and they found that the value of elongation at break was greater in blend films. Xie et al. (2012) also prepared alginate hydrogels containing polyvinyl alcohol (PVA) in different proportions and indicated that the flexibility of the hydrogels increased with increasing PVA concentration. Harper (2013) found that the polysaccharide blend increased tensile stress, while Xie et al. (2012) found that the PVA blend reduced tensile stress. In this study, elevated NAG concentration increased elongation at break and tensile stress values and decreased E-modulus.

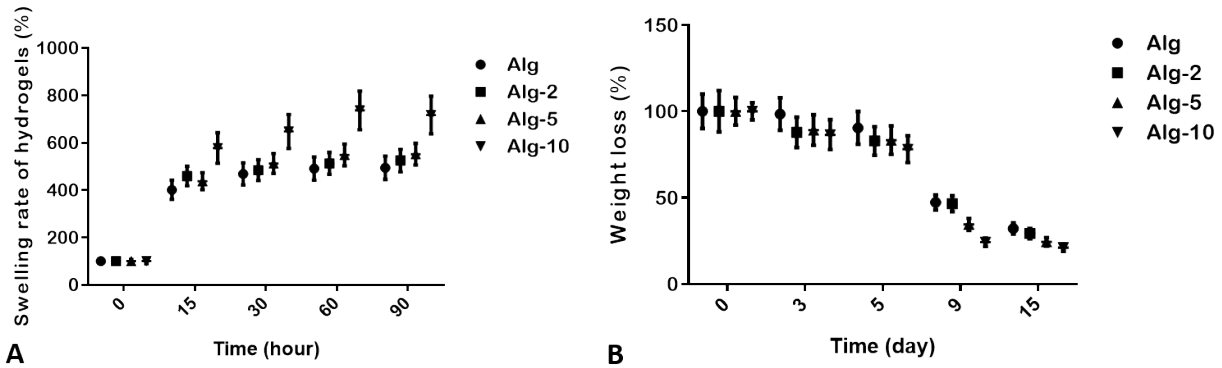

Figure 5. Swelling (A) and degradation (B) properties of hydrogels.

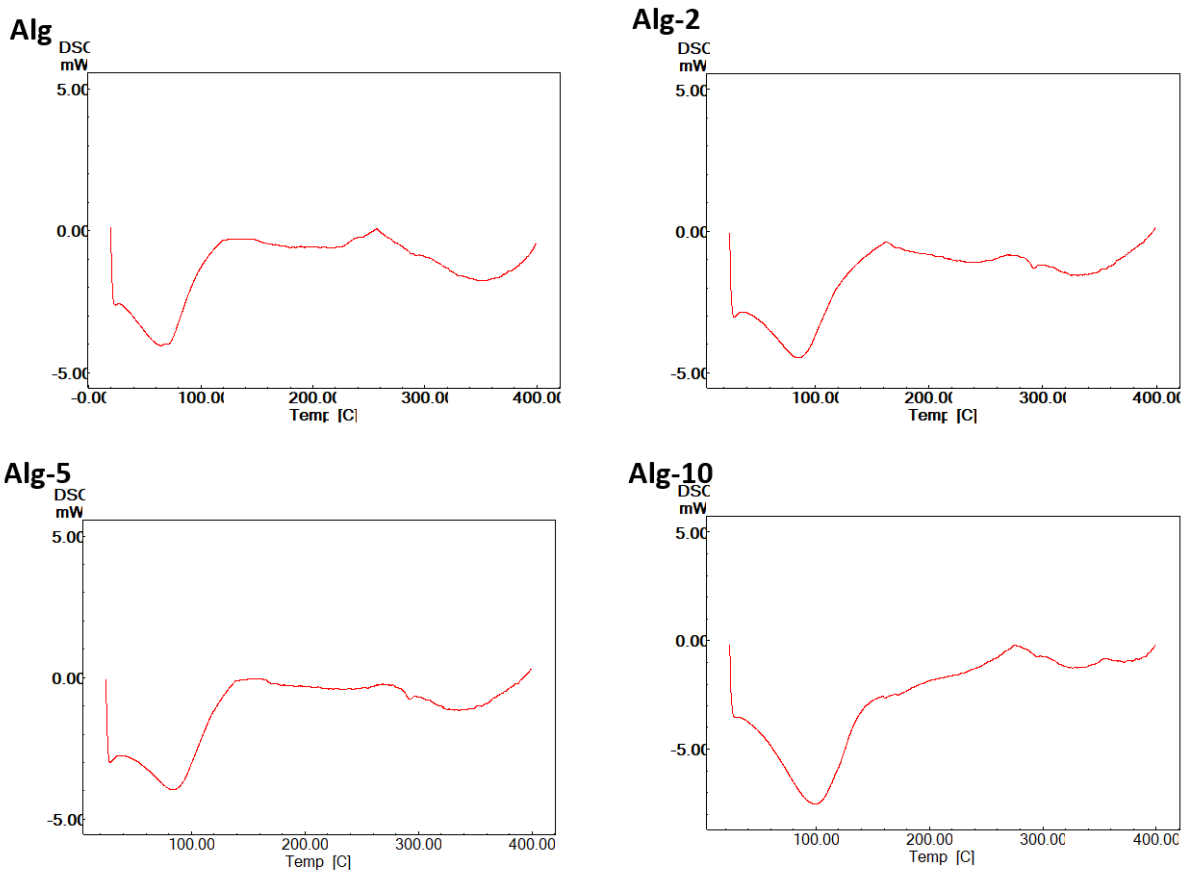

	Dehydration temperature (°C)	Endothermic peak temperature (°C)	Exothermic peak temperature (°C)
Alg	71.73	209.9	258.5
Alg-2	87.88	210.8	277.2
Alg-5	101.34	229.8	276.3
Alg-10	104.46	228.4	280.0

Figure 6. Thermal properties of Alg (A), Alg-2 (B), Alg-5 (C), and Alg-10 (D) hydrogels were determined by DSC experiments.

Table 2. Elongation at break, tensile stress, and E-modulus values of Alg, Alg-2, Alg-5, and Alg-10 hydrogels were determined.

	Elongation at break (%)	Tensile stress (Mpa)	E-modulus (Mpa)
Alg	3.254 ± 1.96	0.098 ± 0.0027	2.57 ± 0.76
Alg-2	3.867 ± 1.63	0.067 ± 0.008	2.3 ± 0.9
Alg-5	4.077 ± 1.51	0.06 ± 0.005	1.95 ± 0.63
Alg-10	8.487 ± 1.47	0.042 ± 0.008	1.03 ± 0.12

3.7. Cytotoxicity studies of hydrogels

The cytotoxicity of hydrogels on human endothelial and human keratinocyte cells was tested via indirect cytotoxicity assay. The study was conducted on 96-well plates and cells treated with standard media were used as control. Extracts from the hydrogels were pipetted onto cultured cells and plates were incubated for 24 h. Cell viability was tested by MTT assay. MTT test results are given in Figures 7A and 7B. According to Rowley et al., (1999) myoblast cells do not adhere on alginate hydrogels, but adhere to and proliferate on alginate hydrogels conjugated with RGD. Dvir-Ginzberg et al. (2003) seeded hepatocytes on alginate hydrogels, and after 7 days they found that cells metabolic activity dropped by 66%. Boeckel et al. (2014) found that the viability of osteoblast cells treated with HA was 74%. Lee et al. (2015) reported that HA at concentrations of 0.1% and 0.3% had little cytotoxicity on corneal epithelial cells and subsequently stimulated epithelial cell proliferation. According to the results, alginate hydrogels have no cytotoxic effect on the cells. Alginate-NAG blend hydrogels stimulate the proliferation of keratinocyte cells about 10%–20% ($P < 0.05$) and endothelial cells about 8%–20% ($P < 0.05$). Cytotoxic effects of NAG-modified alginate were not observed. In contrast, in parallel with the literature, modified alginate sponges stimulated cell proliferation.

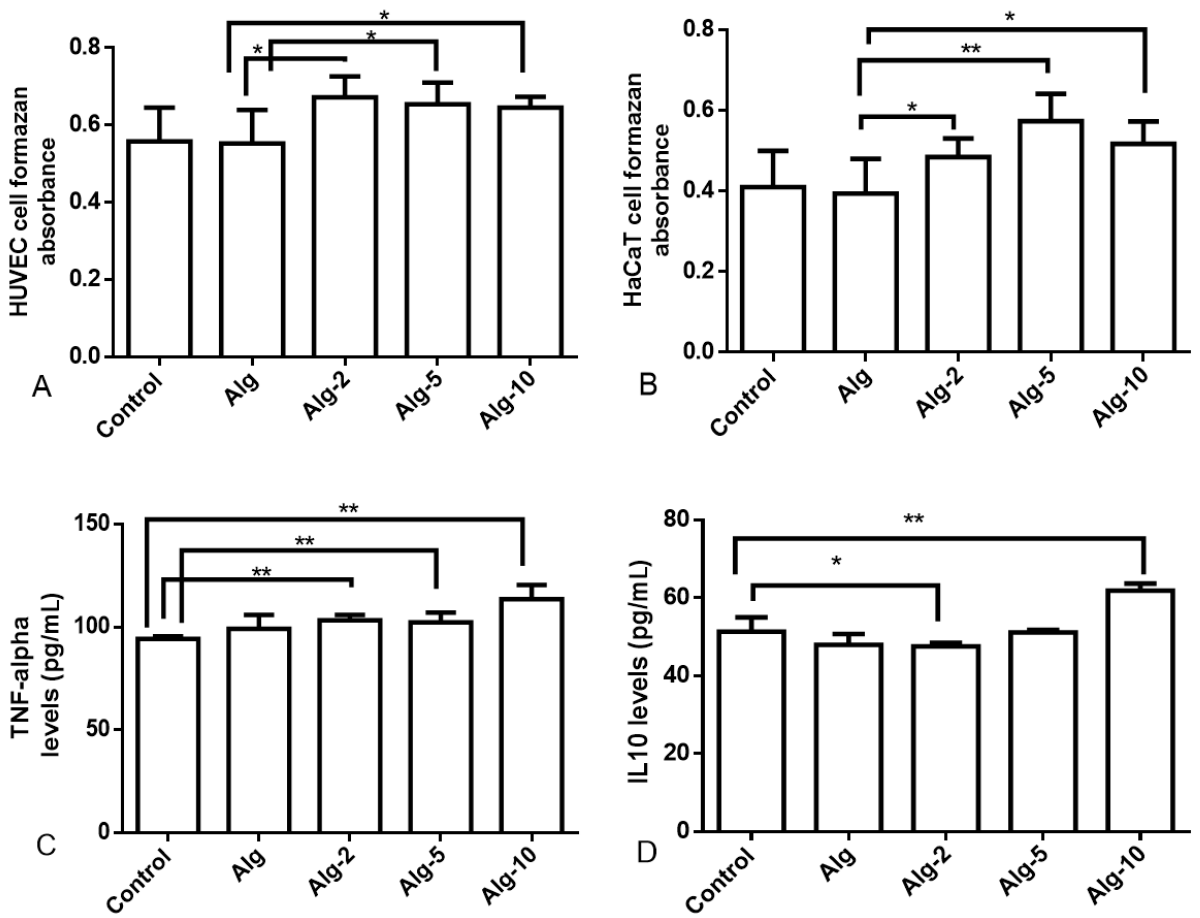

Figure 7. Indirect cytotoxicity of the hydrogels on HUVEC (A) and HaCaT (B) cells was determined. TNF-alpha (C) and IL-10 levels (D) of THP-1 cells interacted with hydrogels were determined.

These results show that alginate and NAG-modified alginate hydrogels have no cytotoxic effects on these cells. Alginate has an inert structure and is not very suitable for new tissue regeneration as a graft without modification. At the same time, the results obtained show that alginate can be used as an active substance carrier matrix, even if it is not modified.

3.8. Cytokine levels of hydrogels

When a dressing material is placed on a wound site, phagocytic cells migrate to the implantation site as a result of the chemokine and cytokine activity of the wound site cells (Franz et al., 2011). One type of the phagocytic cells are macrophages. Macrophages increase or suppress inflammation through cytokines, depending on the physical and chemical properties of material (Boehler et al., 2011). Macrophages belong to either the M1 or M2 phenotype. The M1 phenotype is a phagocytic macrophage and secretes cytokines such as TNF-alpha, IL-1, and IL-6 to increase inflammation. The M2 phenotype produces cytokines such as IL-10 with the goal of suppressing inflammation. Measurement of TNF-alpha and IL-10 cytokine levels of macrophages constitutes an in vitro model of immunological response to biomaterials (Martinez and Gordon, 2014). For this purpose, TNF-alpha and IL-10 levels of hydrogel-treated THP-1 cells were measured using commercial ELISA kits. Cytokine levels are presented in Figures 7C and 7D. According to the results, alginate had no effect on IL-10 and TNF-alpha levels ($P > 0.05$). TNF-alpha and IL-10 levels slightly increased with increasing NAG concentrations. TNF-alpha levels were 94.37 ± 1.19 pg/mL in the control and 113.54 ± 6.94 pg/mL in the Alg-10 hydrogel. IL-10 level was 51.47 ± 3.68 pg/mL in the control group and 61.86 ± 1.84 pg/mL in the Alg-10 hydrogel. The increase in IL-10 and TNF-alpha levels was statistically significant ($P < 0.05$). Noble et al. demonstrated that HA induced TNF-alpha and IL-1β expression in mouse macrophages (1996). They also suggested that HA fragments increase IL-8 gene expression (Noble et al., 1996). McKee et al. (1996) demonstrated that high molecular weight HA has no effect IL-8 gene expression in alveolar macrophages, but low molecular weight HA increases the gene expression .

In conclusion, new hydrogels composed of alginate and NAG were created. The SEM and micro-CT results indicated that the hydrogels had macroporous structure and that these features facilitate gaseous and nutrient exchange for cells. Increasing NAG concentration in alginate hydrogels increased total and open porosity, reduced closed porosity, increased swelling capacity, elongation at break, and tensile stress values, and decreased E-modulus values. The hydrogels had no cytotoxic effect on keratinocytes and endothelial cells, which are the main cells of human skin. Finally, in vitro immunocompatibility studies demonstrated that NAG modification slightly increased TNF-alpha and IL-10 levels. These results indicate NAG-conjugated alginate hydrogels have potential for use as wound-dressing material.

Acknowledgment

This work was supported by the Scientific Research Department of Hacettepe University. The project number is FHD – 2015 - 5348.

References

Asada M, Sugie M, Inoue M, Nakagomı K, Hongo S, Murata K, Tomizuka N (1997). Inhibitory effect of alginic acids on hyaluronidase and on histamine release from mast cells. Biosci Biotech Bioch 61: 1030-1032.

Ates A, Kinikli G, Turgay M, Duman M (2004). The efficacy of viscosupplementation therapy with sodium hyaluronate in patients with knee osteoarthritis. Turk J Geriatr 7: 21-24.

Balakrishnan B, Mohanty M, Umashankar P, Jayakrishnan A (2005). Evaluation of an in situ forming hydrogel wound dressing based on oxidized alginate and gelatin. Biomaterials 26: 6335-6342.

Boeckel DG, Shinkai RSA, Grossi ML, Teixeira ER (2014). In vitro evaluation of cytotoxicity of hyaluronic acid as an extracellular matrix on OFCOL II cells by the MTT assay. Oral Surg Oral Med Oral Pathol Oral Radiol 117: 423-428.

Boehler RM, Graham JG, Shea LD (2011). Tissue engineering tools for modulation of the immune response. Biotechniques 51: 239-244.

Catanzano O, D'esposito V, Acierno S, Ambrosio M, De Caro C, Avagliano C, Ungaro F (2015). Alginate–hyaluronan composite hydrogels accelerate wound healing process. Carbohydr Polym 131: 407-414.

Chang C, Duan B, Zhang L (2009). Fabrication and characterization of novel macroporous cellulose–alginate hydrogels. Polymer 50: 5467-5473.

Chaudhuri O, Gu L, Darnell M, Klumpers D, Bencherif SA, Weaver JC, Mooney DJ (2015). Substrate stress relaxation regulates cell spreading. Nat Commun 6: 7365-7372.

Croce M, Boraldi F, Quaglino D, Tiozzo R, Pasquali-Ronchetti I (2003). Hyaluronan uptake by adult human skin fibroblasts in vitro. Eur J Histochem 47: 63-73.

Croce M, Dyne K, Boraldi F, Quaglino D, Cetta G, Tiozzo R, Ronchetti IP (2001). Hyaluronan affects protein and collagen synthesis by in vitro human skin fibroblasts. Tissue Cell 33: 326-331.

Das D, Pal S (2015). Modified biopolymer-dextrin based crosslinked hydrogels: application in controlled drug delivery. RSC Adv 5: 25014-25050.

Demidova-Rice TN, Hamblin MR, Herman IM (2012). Acute and impaired wound healing: pathophysiology and current methods for drug delivery, part 1: normal and chronic wounds: biology, causes, and approaches to care. Adv Skin Wound Care 25: 304-314.

Draget KI, Skjåk-Bræk G, Smidsrød O (1997). Alginate based new materials. Int J Biol Macromol 21: 47-55.

Dvir-Ginzberg M, Gamlieli-Bonshtein I, Agbaria R, Cohen S (2003). Liver tissue engineering within alginate scaffolds: effects of cell-seeding density on hepatocyte viability, morphology, and function. Tissue Eng 9: 757-766.

Franz S, Rammelt S, Scharnweber D, Simon JC (2011). Immune responses to implants–a review of the implications for the design of immunomodulatory biomaterials. Biomaterials 32: 6692-6709.

Fundueanu G, Nastruzzi C, Carpov A, Desbrieres J, Rinaudo M (1999). Physico-chemical characterization of Ca-alginate microparticles produced with different methods. Biomaterials 20: 1427-1435.

Grellner W, Georg T, Wilske J (2000). Quantitative analysis of proinflammatory cytokines (IL-1β, IL-6, TNF-α) in human skin wounds. Forensic Sci Int 113: 251-264.

Harper BA (2013). Understanding interactions in wet alginate film formation used for in-line food processes. PhD Thesis, University of Guelph, Ontario, Canada.

Hashimoto T, Suzuki Y, Tanihara M, Kakimaru Y, Suzuki K (2004). Development of alginate wound dressings linked with hybrid peptides derived from laminin and elastin. Biomaterials 25: 1407-1414.

Hsu SH, Whu SW, Hsieh SC, Tsai CL, Chen DC, Tan TS (2004). Evaluation of chitosan-alginate-hyaluronate complexes modified by an RGD-containing protein as tissue-engineering scaffolds for cartilage regeneration. Artif Organs 28: 693-703.

Jahn M, Baynes JW, Spiteller G (1999). The reaction of hyaluronic acid and its monomers, glucuronic acid and N-acetylglucosamine, with reactive oxygen species. Carbohydr Res 321: 228-234.

Kaklamani G, Cheneler D, Grover LM, Adams MJ, Bowen J (2014). Mechanical properties of alginate hydrogels manufactured using external gelation. J Mech Behav Biomed Mater 36: 135-142.

Kataria K, Gupta A, Rath G, Mathur R, Dhakate S (2014). In vivo wound healing performance of drug loaded electrospun composite nanofibers transdermal patch. Int J Pharm 469: 102-110.

Kim JO, Park JK, Kim JH, Jin SG, Yong CS, Li DX, Lyoo WS (2008). Development of polyvinyl alcohol–sodium alginate gel-matrix-based wound dressing system containing nitrofurazone. Int J Pharm 359: 79-86.

Komine M, Rao LS, Kaneko T, Tomic-Canic M, Tamaki K, Freedberg IM, Blumenberg M (2000). Inflammatory versus proliferative processes in epidermis tumor necrosis factor α induces k6b keratin synthesis through a transcriptional complex containing NFκB and C/EBPβ. J Biol Chem 275: 32077-32088.

Laus R, Costa TG, Szpoganicz B, Fávere VT (2010). Adsorption and desorption of Cu (II), Cd (II) and Pb (II) ions using chitosan crosslinked with epichlorohydrin-triphosphate as the adsorbent. J Hazard Mater 183: 233-241.

Lee JS, Lee SU, Che CY, Lee JE (2015). Comparison of cytotoxicity and wound healing effect of carboxymethylcellulose and hyaluronic acid on human corneal epithelial cells. Int J Ophthalmol 8: 215-221.

Lee KY, Mooney DJ (2012). Alginate: properties and biomedical applications. Prog Polym Sci 37: 106-126.

Li Z, Ramay HR, Hauch KD, Xiao D, Zhang M (2005). Chitosan–alginate hybrid scaffolds for bone tissue engineering. Biomaterials 26: 3919-3928.

Maia F, da Silva J, do Amaral F, Martin A, Lobo A, Soares L (2013). Morphological and chemical evaluation of bone with apatite-coated Al2O3 implants as scaffolds for bone repair. Cerâmica 59: 533-538.

Martinez FO, Gordon S (2014). The M1 and M2 paradigm of macrophage activation: time for reassessment. F1000Prime Rep 6: 12703-12728.

McKee CM, Penno MB, Cowman M, Burdick MD, Strieter RM, Bao C, Noble PW (1996). Hyaluronan (HA) fragments induce chemokine gene expression in alveolar macrophages. The role of HA size and CD44. J Clin Invest 98: 2403-2416.

Mohan N, Nair PD (2005). Novel porous, polysaccharide scaffolds for tissue engineering applications. Trends Biomater Artif Organs 18: 219-224.

Noble PW, McKee CM, Cowman M, Shin HS (1996). Hyaluronan fragments activate an NF-kappa B/I-kappa B alpha autoregulatory loop in murine macrophages. J Exp Med 183: 2373-2378.

Olutoye OO, Cohen IK (1996). Fetal wound healing: an overview. Wound Repair Regen 4: 66-74.

Rowley JA, Madlambayan G, Mooney DJ (1999). Alginate hydrogels as synthetic extracellular matrix materials. Biomaterials 20: 45-53.

Sarmento B, Ferreira D, Veiga F, Ribeiro A (2006). Characterization of insulin-loaded alginate nanoparticles produced by ionotropic pre-gelation through DSC and FTIR studies. Carbohydr Polym 66: 1-7.

Sheehan KM, DeLott LB, West RA, Bonnema JD, DeHeer DH (2004). Hyaluronic acid of high molecular weight inhibits proliferation and induces cell death in U937 macrophage cells. J Life Sci 75: 3087-3102.

Simmons CA, Alsberg E, Hsiong S, Kim WJ, Mooney DJ (2004). Dual growth factor delivery and controlled scaffold degradation enhance in vivo bone formation by transplanted bone marrow stromal cells. Bone 35: 562-569.

Sinha M, Banik RM, Haldar C, Maiti P (2013). Development of ciprofloxacin hydrochloride loaded poly (ethylene glycol)/ chitosan scaffold as wound dressing. J Porous Mater 20: 799-807.

Soares J, Santos J, Chierice G, Cavalheiro E (2004). Thermal behavior of alginic acid and its sodium salt. Eclet Quím 29: 57-64.

Straccia MC, d'Ayala GG, Romano I, Oliva A, Laurienzo P (2015). Alginate hydrogels coated with chitosan for wound dressing. Mar Drugs 13: 2890-2908.

Trif M, Ansorge-Schumacher M, Socaciu C (2007). Application of FTIR Spectroscopy for determination of oxidation of encapsulated sea buckthorn oil. XVth International Workshop on Bioencapsulation. Vienna, Austria, pp. 3-7.

Unemori E, Hibbs M, Amento E (1991). Constitutive expression of a 92-kD gelatinase (type V collagenase) by rheumatoid synovial fibroblasts and its induction in normal human fibroblasts by inflammatory cytokines. J Clin Invest 88: 1656-1662.

Walker M, Hobot J, Newman G, Bowler P (2003). Scanning electron microscopic examination of bacterial immobilisation in a carboxymethyl cellulose (AQUACEL®) and alginate dressings. Biomaterials 24: 883-890.

Wallace HJ, Stacey MC (1998). Levels of tumor necrosis factor-α (TNF-α) and soluble TNF receptors in chronic venous leg ulcers–correlations to healing status. J Invest Dermatol 110: 292-296.

Werner S, Peters KG, Longaker MT, Fuller-Pace F, Banda MJ, Williams LT (1992). Large induction of keratinocyte growth factor expression in the dermis during wound healing. Proc Natl Acad Sci 89: 6896-6900.

Wiegand C, Heinze T, Hipler UC (2009). Comparative in vitro study on cytotoxicity, antimicrobial activity, and binding capacity for pathophysiological factors in chronic wounds of alginate and silver-containing alginate. Wound Repair Regen 17: 511-521.

Xie L, Jiang M, Dong X, Bai X, Tong J, Zhou J (2012). Controlled mechanical and swelling properties of poly (vinyl alcohol)/ sodium alginate blend hydrogels prepared by freeze–thaw followed by Ca^{2+} crosslinking. J Appl Polym Sci 124: 823-831.

Zhang C, Jia Z (2010). Preparation of porous chitosan microsphere absorbent and research on its absorption ability for Cu^{2+} and Zn^{2+}. International Journal of Chemistry 2: 113-120.